Impact of nitrogen seeding on the AUG pedestal: experiments and modelling

M. G. Dunne[1], L. Frassinetti[2], M. Beurskens[3], M. Cavedon[1,4], R. Fischer[1], G.T.A. Huijsmans[5], F. M. Laggner[6], R. M. McDermott[1], G. Tardini[1], E. Viezzer[1], E. Wolfrum[1], the EUROfusion MST1 Team*and the ASDEX-Upgrade Team[1]

[1]*Max-Planck-Institut für Plasmaphysik, D-85748 Garching,Germany*

[2]*Division of Fusion Plasma Physics, Association EURATOM-VR, KTH, SE-10044 Stockholm, Sweden*

[3]*EURATOM/CCFE Fusion Association, Culham Science Centre, Abingdon, OX14 3DB,UK*

[4]*Physik-Department E28, Technische universität München, Garching Germany*

[5]*ITER Organization, Route de Vinon sur Verdon, F-13115 St Paul Lez Durance, France*

[6]*Institute of Applied Physics, TU Wien, Fusion@ÖAW, 1040 Vienna, Austria*

Introduction

Improved confinement with nitrogen seeding has been widely reported on AUG and JET in recent years [1, 2]. However, despite intensive experimental and theoretical investigation on both devices, an explanation for this phenomenology has thus far remained elusive. One currently working hypothesis [3] for this effect starts with the assumption of a peeling-ballooning limited pedestal. When nitrogen is seeded, the edge current density is transiently reduced by the increased Z_{eff}, allowing access to a higher pedestal pressure gradient. This then propagates into a higher thermal energy in the core plasma, which in turn acts to further stabilise the pedestal via an increased Shafranov shift.

A set of experiments were carried out during the last AUG experimental campaign with the aim of experimentally testing this hypothesis and providing data for modelling. Testing of such a hypothesis involves both interpretive and predictive modelling components to verify the above mechanism.

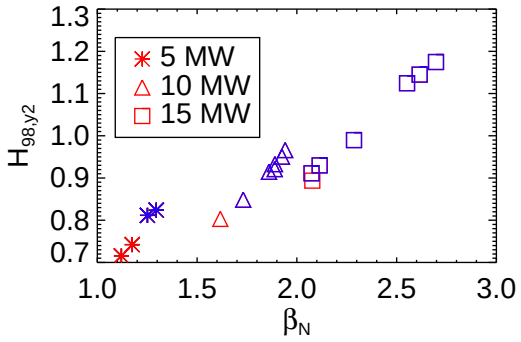

Figure 1: Normalised confinement time plotted against normalised plasma beta. These two measures of the plasma stored energy increase with increasing heating power (different symbols) and impurity seeding (blue symbols).

Experiments

The experiments were carried out in a similar configuration to the scenario where the highest confinement improvement (40%) [1] was observed on AUG; 1 MA plasma current, -2.5 T toroidal magnetic field, medium triangularity (δ_{av}~0.25), with a deuterium gas puff of $2.7-3.0\times10^{22}$electronss^{-1}. Three power levels

*see http://www.euro-fusionscipub.org/mst1

were used to investigate any beta dependence and also to investigate the behaviour of unseeded pedestals in response to a higher core beta. The additional neutral beam injection (NBI) power was varied from 5-10-12.5 MW. At the highest level of input NBI power, an additional 2 MW of ICRH power were also applied. A constant ECRH power of 1 MW was applied in the core of all discharges to prevent impurity accumulation. An overview of the confinement in these discharges is shown in a $H_{98,y2}$-β_N plot in figure 1.

Both measures of the plasma stored energy increase with increasing heating power and also with increasing impurity seeding level. The highest levels of confinement improvement obtained were 8, 15 and 25 % in the low, medium, and high input power discharges, respectively.

Only low levels of nitrogen seeding could be applied at the lowest heating power to avoid outer divertor detachment; this causes a large increase of the plasma density, changing the confinement regime significantly. Althought the highest confinement is reached with the highest input power and the highest level of nitrogen seeding, it is difficult to separate these two effects as less nitrogen seeding could be applied at the lower power levels.

Figure 2 shows the normalised plasma beta as a function of pedestal top temperature. A strong dependence of the stored energy on the temperature is observed, while the density pedestal (not shown) has only a minor role in confinement changes, consistent with previous results [1, 4, 5]. From the different behaviour of the temperature and density pedestals, we can creates a picture of two constraints on the AUG pedestals; one on the density pedestal, which recovers first after the ELM crash in most AUG scenarios [6], and, ultimately, a peeling-ballooning limited pressure pedestal.

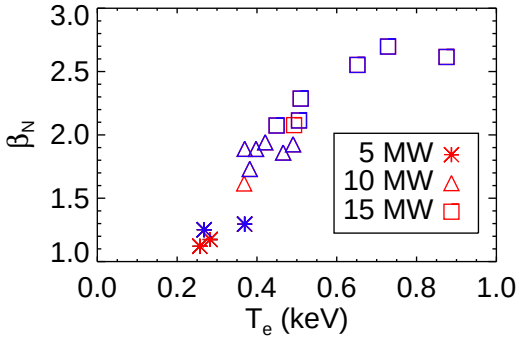

Figure 2: Normalised plasma beta plotted as a function of pedestal top electron temperature, showing a dominant role of the electron temperature in the stored energy increases in this databae.

In order to further vary the range of pedestal top parameters, a triangularity scan was also performed as part of this discharge set. An overview of the pedestal parameters for both shapes, with and without impurity seeding, is shown in figure 3. Circles denote the low triangularity ($\delta_{av} = 0.25$) portions of these discharges, with triangles showing data from the high triangularity ($\delta_{av} = 0.35$) phases. Red indicates an unseeded reference discharge, blue shows the seeded counterparts. The increasing levels of fill indicate increasing power levels. Only one seeding level was performed for each heating step in these discharges. Also shown is a comparison discharge with methane (CD_4) puffing with both low and high triangularity phases (see [7] for more

information).

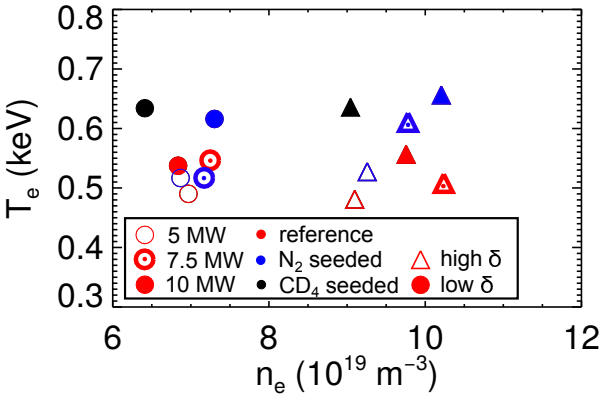

Figure 3: Pedestal top temperature as a function of pedestal top density for low (circles) and high (triangles) plasma shaping, with three heating levels (different fill levels) and with (blue) and without (red) impurity seeding). A discharge with CD_4 puffing is also shown in black.

Three key pieces of information regarding these AUG scenarios are shown in this figure: 1) increasing triangularity always increases the pedestal top in contrast with JET baseline discharges; 2) CD_4 has a comparable effect to N_2[7] and; 3) impurity seeding acts *only* on the temperature pedestal while plasma shaping acts *only* on the density pedestal. While prediction of the pedestal top density requires significant theory development to understand, predicting the combined pressure pedestal height should be within the capabilities of present day peeling-ballooning (PB) theory.

Modelling

Within the framework of PB, a predictive model was used to vary the plasma beta, shape, and impurity content in a controlled fashion not accessible in the experiment. To perform these variations, sample profiles were created in the same manner as in the EPED model [8], i.e. the pedestal top density is specified and the temperature height is varied to provide the different test pressure pedestal heights. The pedestal width was determined using the $\sqrt{\beta_{\mathrm{pol,ped}}}$ scaling [8]. The current density was then calculated using the Sauter model [9] for the bootstrap current and neoclassical resistivity. The toroidal electric field was assumed to be constant over the plasma radius and used to scale the Ohmic current density until the desired plasma current was reached.

The stability of each of these pressure-current density profile pairs was then tested for a sample of mode numbers ($1 < n < 70$) using the MISHKA-fast code, which is a variant of the MISHKA-1 code [10] which analyses a radially dependent array of poloidal mode numbers depending on the local q value. The results of this modelling are shown in figure 4.

The red solid line indicates the predicted total pressure ($p_i + p_e$) pedestal top as a function of plasma beta at low triangularity and a Z_{eff} of 1.3, while the blue solid line shows the same for the high triangularity shape used in this work. The dashed lines correspond to simulations with a Z_{eff} of 2.

Several key results are presented in this figure. First, the code predicts that, for this parameter set, increasing the plasma shaping will always result in an increase of the pedestal top. This was observed in the experiments, where the pedestal top increased even at the lowest input power. Secondly, at high beta, the increase of the pedestal top as a function of global beta saturates; this

is due to the pedestal moving from a ballooning limited to a peeling limited regime. Different experimental conditions with, for example, a low beta operational point at low current density and pressure gradient, as is the case for JET BL plasmas, may not see this saturation over the available range of global beta. Thirdly, the model does predict an increased pedestal top with an increased Z_{eff}.

However, the magnitude of this increase (~5%) is significantly lower than in the experiment, and in the low triangularity shape and at low beta, the model predicts a *decrease* of confinement, which is not observed in experiments on either AUG or JET before the plasma transitions to a Type-III ELMing regime. This indicates that there is an (are) additional physics mechanism(s) at play other than the impact of Z_{eff} on the edge current density alone.

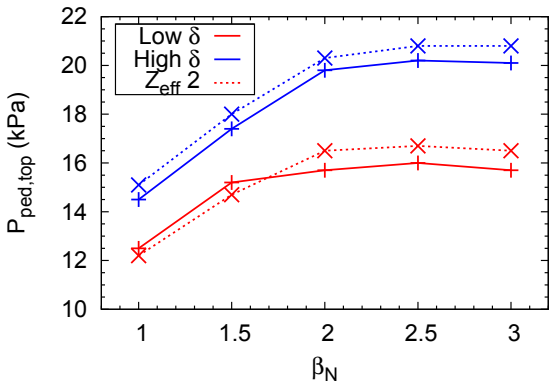

Figure 4: Predicted pedestal top as a function of plasma beta for low (red) and high (blue) triangularity with Z_{eff} of 1.3 (solid) and 2.0 (dashed).

Conclusions

A series of experiments on AUG has revealed that impurity seeding increases the plasma stored energy by increasing the temperature pedestal. Experiments at high triangularity have shown a separation of the impact of shaping and seeding on the density and temperature pedestals, respectively. Predictive modelling of these effects shows that the effect of triangularity on pedestal pressure is clear. However, the same modelling demonstrates that the change in Z_{eff} in the pedestal and its corresponding impact on the bootstrap current does not give rise to the observed increases; further analysis taking the effects of divertor radiation into account in some manner (such as a change of the separatrix temperature) is likely to be required to explain these effects on stability.

References

[1] A. Kallenbach, et al. *Plasma Physics and Controlled Fusion*, 55(12), 2013.

[2] C. Giroud, et al. *Nuclear Fusion*, 53(11), 2013.

[3] M G Dunne, et al. In *41st EPS Conference on Plasma Physics*, Berlin, 2014.

[4] J. Schweinzer, et al. *Nuclear Fusion*, 51(11), 2011.

[5] G Tardini, et al. *Plasma Physics and Controlled Fusion*, 55(1), 2013.

[6] A. Burckhart, et al. *Plasma Physics and Controlled Fusion*, 52(10), 2010.

[7] M.N.A. Beurskens, et al. In *42nd EPS Conference on Plasma Physics*, Lisbon, 2015.

[8] P.B. Snyder, et al. *Nuclear Fusion*, 49(8), 2009.

[9] O. Sauter, et al. *Physics of Plasmas*, 6(7), 1999.

[10] A. B. Mikhailovskii, et al. *Plasma Physics Reports*, 23, 1997.

This work has been carried out within the framework of the EUROfusion Consortium and has received funding from the Euratom research and training programme 2014-2018 under grant agreement No 633053. The views and opinions expressed herein do not necessarily reflect those of the European Commission.